University of Nevada, Reno

Chemical Modulation of Slit Proteolysis by Tolloid-like 1

A thesis submitted in partial fulfillment of the requirements
for the degree of Master of Science in Neuroscience

by

Mary Weatherbee Sorcher

Dr. Thomas Kidd/Thesis Advisor

May 2021

THE GRADUATE SCHOOL

We recommend that the thesis prepared under our supervision by

Mary Weatherbee Sorcher

entitled

Chemical Modulation of Slit Proteolysis by Tolloid-like 1

be accepted in partial fulfillment of the

requirements for the degree of

Master of Science

Thomas Kidd, Ph.D., *Advisor*

Michael Webster, Ph.D., *Committee Member*

Michael Teglas, D.V.M, Ph.D., *Graduate School Representative*

David W. Zeh, Ph.D., *Dean*, *Graduate School*

May 2021

Abstract

Slits are large secreted proteins that repel growing axons during nervous system development, primarily by binding Roundabout (Robo) receptors. In addition to axon guidance, Slit-Robo signaling is linked to a wide range of biological processes including cell migration, angiogenesis, and cancer metastasis. The full-length Slit protein (Slit-FL) is proteolytically cleaved into two functionally distinct fragments, Slit-N and Slit-C. The Slit-N fragment has been identified for its therapeutic potential in multiple disease pathologies with diverse beneficial effects such as increasing vascular stability and promoting neuronal survival and outgrowth. Accurately identifying the Slit protease is paramount for understanding Slit processing and necessary for targeting the protease for modulation to therapeutically increase availability of Slit-N. Here we provide evidence to support that the metalloprotease Tolloid-like 1 (Tll1) is the direct protease of Slit, not prohormone convertases as other labs have previously proposed. Furthermore, we propose a pharmacological strategy to indirectly activate Tll1 as a mechanism for increasing Slit-N levels in microbially infected endothelial and lung cells. This therapeutic potential speaks to the critical need for effective strategies to treat SARS-CoV-2-related vascular and lung damage.

Acknowledgements

I am grateful to our collaborators S. Verma and T. Uppal for providing and managing the A549 cells and HUVECs and for their expertise and insight. I thank B. Bae and P. Muira for providing mESC-derived glutamatergic neurons, L. Jones and G. Mastick for assistance with Cos-7 cell culture, and M. Song and X. Huang for their work in the Kidd laboratory characterizing Tll1 proteolytic activity. Thank you to R. Kellermeyer for support that knows no bounds and to T. Kidd for invaluable guidance and mentorship.

Funding

This work was supported by grants from the National Institutes of Health (1R56NS114219) and by the National Institute of General Medical Sciences of the National Institutes of Health (P20 GM103650).

Introduction

Slits are large, highly conserved secreted proteins that are critical for proper axon guidance during neurodevelopment. Through interactions with Roundabout (Robo) receptors, they repel growing axons from the CNS midline (Howard et al., 2019). In addition to axon guidance, Slit-Robo signaling is linked to a wide range of biological processes including neurogenesis, angiogenesis, and cancer metastasis (Blockus and Chedotal, 2016). Control of Slit-signaling is mediated through receptor function and by proteolytic processing. Full-length Slit (Slit-FL) is proteolytically cleaved into two functionally distinct fragments, N-terminal Slit (Slit-N) and C-terminal Slit (Slit-C) (Figure 1A; Brose et al., 1999; Nguyen Ba-Charvet et al., 2001; Wang et al., 1999). Slit2-N is widely thought to be the active signaling molecule, because like Slit2-FL, it binds Robo receptors. However, Slit2-N has been shown to bind different receptors from Slit-FL, such as Dscam1, and act antagonistically to Slit2-FL in different contexts (Kellermeyer et al., 2020). Slit2-N demonstrates a functionally distinct role from Slit2-FL in its growth promotion of longitudinal axons (Alavi et al., 2016). The function of Slit2-C is still undetermined, but it is implicated in thermogenesis regulation, axon repulsion via Plexin receptors and, unlike Slit2-FL and Slit2-N, it is not tightly associated with the cell surface. (Brose et al., 1999; Delloye-Bourgeois et al., 2015; Svensson et al., 2016). The variability of signals and responses Slit can elicit depending on its cleaved or uncleaved state makes identifying the Slit protease crucial for understanding Slit signaling regulation.

The Slit protease in *Drosophila* was recently identified as the zinc metalloprotease Tolkin (Tok) by the Kidd laboratory (Kellermeyer *et al.*, 2020). Preliminary data suggests that Tolloid-like 1 (Tll1), a Tok homolog, is the vertebrate Slit protease (X. Huang & M. Song, 2019 unpublished results). Like Tok, Tll1 belongs to the bone morphogenetic protein-1 (BMP1) and tolloid-like proteinase family which cleave secreted proteins, especially growth factors and collagens. (Troilo et al., 2016). Tll1 is activated by the removal of its inhibitory prodomain by a Furin-like prohormone convertase (Figure 1B; Scott et al., 1999). It has been suggested previously that *Drosophila* Slit is cleaved by the prohormone convertase Amontillado (Amon) (Ordan and Volk, 2016). The Kidd laboratory was unable to repeat these results (Kellermeyer *et al.*, 2020). In vertebrates, Slit2 is not cleaved in the presence of the Furin prohormone convertase inhibitor chloromethylketone (CMK) (Ducuing et al., 2020). We hypothesize that Slit2 is not cleaved under these conditions because the inhibition of prohormone convertases is preventing Tll1, the direct Slit protease, from becoming activated. In an attempt to replicate previous work, we were unable to inhibit Slit2 cleavage with CMK. However, we do demonstrate that our activated Tll1 construct, Tll1 that has been modified with a deletion of its inhibitory prodomain, does appear to be biologically active regardless of the presence of CMK *in vitro.*

The Slit2-N fragment has been identified for its therapeutic potential in multiple disease pathologies due to beneficial effects such as increasing vascular stability and promoting neuronal survival and outgrowth (London and Li, 2011; London et al., 2010; Piper et al., 2002). In mouse models of H5N1 (avian flu) infection, Slit2-N treatment improves vascular resilience in

response to cytokine storm and decreases mortality rate (London et al., 2010). Slit2-N's potential as a therapeutic for virally induced Acute Respiratory Distress Syndrome (ARDS) is particularly pertinent during the current SARS-CoV-2 pandemic. Like H5N1-related ARDS, SARS-CoV-2-related ARDS is a severe lung inflammatory disorder characterized by vascular leakage and cytokine storm (Gonzalez et al., 2015, London et al., 2010). There is a 90% incidence rate of ARDS among non-survivors of SARS-CoV-2 infection (Tzotzos et al., 2020). The main clinical treatment is mechanical ventilation and effective pharmacological interventions are limited. (Gonzalez et al., 2015). Activation of the Slit2 protease to increase levels of Slit2-N presents a potential therapeutic strategy.

NR4A1 (nuclear receptor subfamily 4 group A member 1, also known as Nur77) is a regulator of gene expression in inflammation and of interest for its potential role in the pathogenesis of ARDS (Jiang et al, 2016). The vertebrate Slit protease Tll1 was identified as a gene that is induced greater than 5-fold by expression of NR4A1. (Chao et al, 2008) Pharmacological activation of NR4A1 by the drug Cytosporone B (CsnB) has been demonstrated to inhibit inflammatory endothelin-1 expression in ARDS model rats, decrease LPS-induced phosphorylation of NF-κB and p38 MAPK, and relieve lung, liver, and kidney injury (Jiang et al, 2016) CsnB is a NR4A1 agonist and results in being translocated to the nucleus (Zhan et al., 2008). NR4A1 also acts in the cytoplasm to alieve inflammation by an independent mechanism which is enhanced by the drug Celastrol (Hu et al., 2017). 6-Mercaptopurine (6-MP) is a well-established immunosuppressant that enhances NR4A1 expression (Huang et al., 2016). Using an *in vitro* model, we investigate the use of NR4A1 agonists to indirectly upregulate Slit2-N and

propose this mechanism as a potential pharmacological approach to treat pulmonary and vascular damage in SARS-CoV-2-related ARDS.

Results

Generation of a constitutively active Tll1 construct

The prohormone convertase inhibitor CMK has been reported to inhibit Slit2 cleavage (Ducuing et al., 2020). We hypothesized that CMK is actually preventing activation of the protease Tll1 by preventing removal of its inhibitory domain by a Furin-like prohormone convertase. **We hypothesized that an activated Tll1 protease would be able to cleave Slit2 in the presence of CMK proving the effect of prohormone convertases as indirect and identifying Tll1 as the direct protease of Slit2.** To test this, we generated an activated Tll1 construct (aTll1, Figure 1B). The N-terminal end of the active Tll1 has been sequenced and the cleavage site identified, strongly suggesting that as a Furin-like prohormone convertase is the likely protease (Scott et al., 1999). We designed primers to delete the inhibitory prodomain defined by Scott et al. using an In-Fusion cloning approach (TakaraBio). In brief, PCR primers were designed to amplify a human Tll1 clone with a FLAG epitope tag in the pcDNA3.1+/C-(K)-DYK vector to generate a linear PCR product lacking the inhibitory prodomain. The primers contained 15 base overlaps that allowed recircularization of the PCR product and transformation into bacteria. Clone identity was validated by sequencing. The construct was further validated by expression in Cos-7 cells and protein levels were visualized by Western blotting with a Tll1 antibody. Compared to

the wild-type protein, activated Tll1 protein showed a reduction in size corresponding to the 348bp/116aa deletion of the inhibitory prodomain (Fig. 1C).

Figure 1.

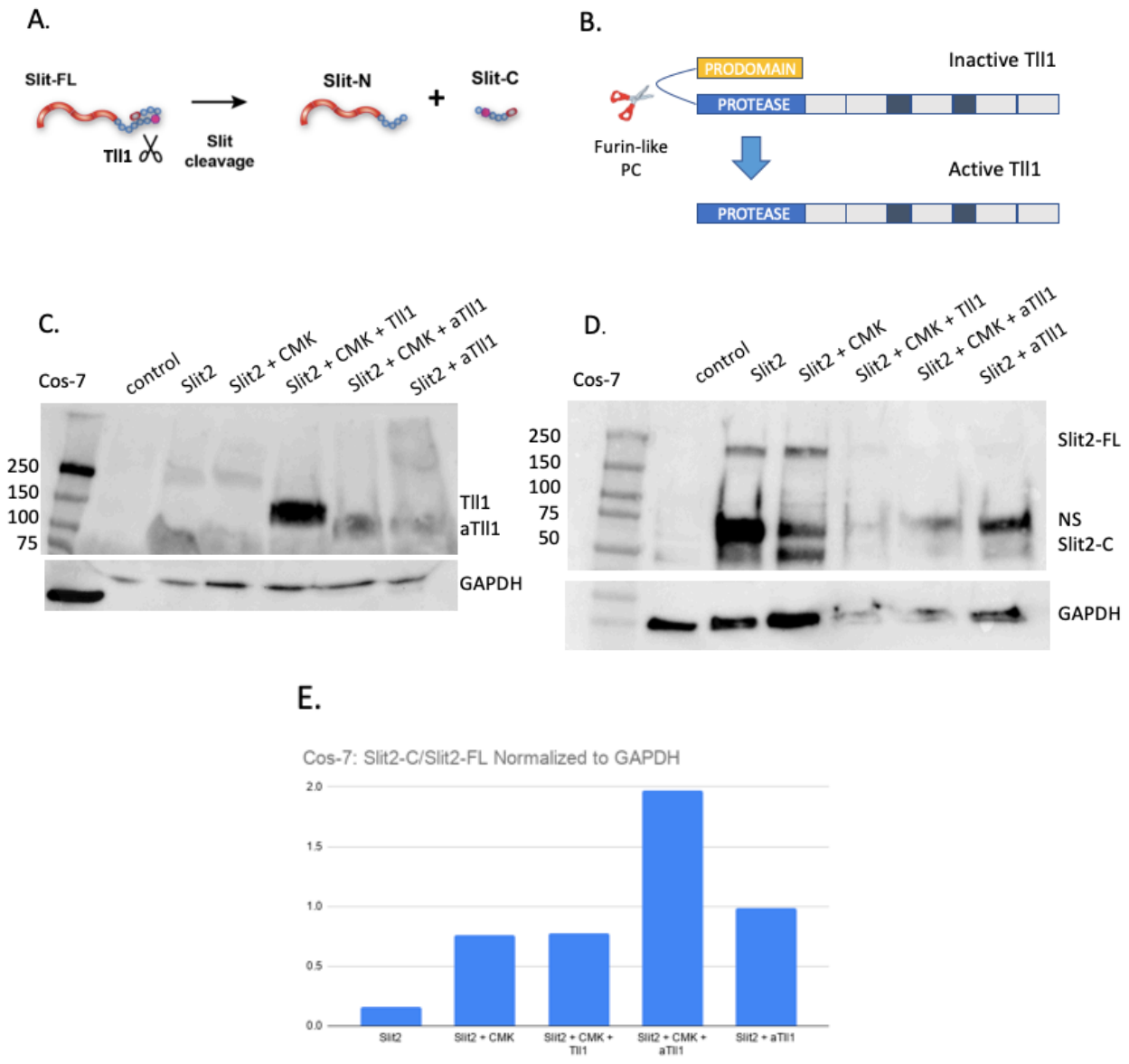

Figure 1. (A) Slit2-FL is proteolytically cleaved by Tll1 into two functionally distinct fragments: Slit2-N and Slit2-C. **(B)** Tll1 is activated by cleavage of its inhibitory prodomain. A Furin-like prohormone convertase (PC) is the likely Tll1 protease (Scott et al., 1999). **(C-D)** Cos-7 bone

carcinoma cells were transfected with plasmids encoding for full-length Slit2 (Slit2) alone or co-transfected with either Tll1 or activated Tll1 (aTll1) encoding plasmids. Transfected cells were treated with prohormone convertase inhibitor CMK to test the effects of PC inhibition on Slit2 proteolysis. We hypothesized that aTll1 would cleave Slit2 in the presence of CMK, but Tll1, which requires a Furin-like PC to be activated, would not. This would prove that the effects of PCs are indirect to Slit2 cleavage and identify Tll1 as the direct Slit2 protease. **(C)** Western blot of cell supernatants labeled with a polyclonal antibody for Tll1 shows successful transfection of Tll1 at ~114kD and aTll1 at ~101kD (visible in the lanes transfected with Tll1/aTll1). The ~13kD decrease in size of aTll1 compared to Tll1 is consistent with our 116 amino acid deletion of the inhibitory prodomain. **(D)** Western blot of cell supernatants labeled with a monoclonal antibody for Slit2-C shows a surprising increase in Slit2 cleavage in the presence of CMK. Slit2-FL is the upper band at ~180kD and Slit2-C is the lower band at ~55kD. Unexpected non-specific (NS) band at ~70kD appears to be associated with Slit2-C. **(E)** Quantification of Slit2 processing, measured as a ratio of relative pixels of Slit2-C compared to Slit2-FL normalized to loading control GAPDH, shows increased Slit2 cleavage in the presence of CMK with the highest levels of Slit2 cleavage in aTll1 transfected cells. However, due to faint bands in all lanes transfected with Tll1/aTll1, the accuracy of this quantification is unreliable.

Evaluating the Effects of CMK on Slit2 Proteolysis

To test the effect of CMK on Slit2 proteolysis, we expressed Slit2 in Cos-7 cells in the presence and absence of CMK. Cos-7 cells do not normally express Slit2, so we transfected the cells with plasmids encoding for full-length Slit2. We detected Slit2 expression in the cell media using a monoclonal Slit2-C antibody. Cos-7 cells have an endogenous Slit2 cleavage activity which is attributed to a currently unidentified protease (Kellermeyer, 2020; Fig. 1C, 1D). A previous study has shown that adding CMK after transfection inhibits Slit2 cleavage (Ducuing, 2020). However, we found that CMK instead appeared to increase the amount of Slit2 proteolysis (n=1, Fig. 1D) which was confirmed by quantification (Fig. 1E). In a second experiment, there was insufficient endogenous cleavage of Slit2 to judge proteolysis. The report of CMK inhibiting Slit2 cleavage used N2A cells and a different antibody to detect cleavage (Ducuing, 2020). The

difference in cell type may be responsible for the discrepancy (see discussion). The observations warrant further investigation.

Testing aTll1 in Cell Culture

Despite the contrary effect of CMK in Cos-7 cells, we compared the ability of Tll1 and aTll1 to cleave Slit2. In previous experiments in the Kidd laboratory, expression of the Tll1 protease has been repeatedly observed to lead to degradation of Slit2 (X. Huang & M. Song, 2019 unpublished results). Even in the presence of CMK, we observed this substrate degradation phenomenon by both Tll1 and aTll1 (Fig. 1D; n=2). Experiments are ongoing to titrate the ratio of protease and substrate to mitigate this effect. Based on the presence of Slit2-C and degradation of the Slit2 substrate, we find that aTll1 is a functional protease capable of cleaving Slit2. Resolution of the effect of CMK on Slit2 proteolysis in transfected Cos-7 cells awaits further investigation. Quantification of the ratio between Slit2-C and Slit2-FL expression was performed but due to the faintness of the bands, these results are unreliable.

Figure 2.

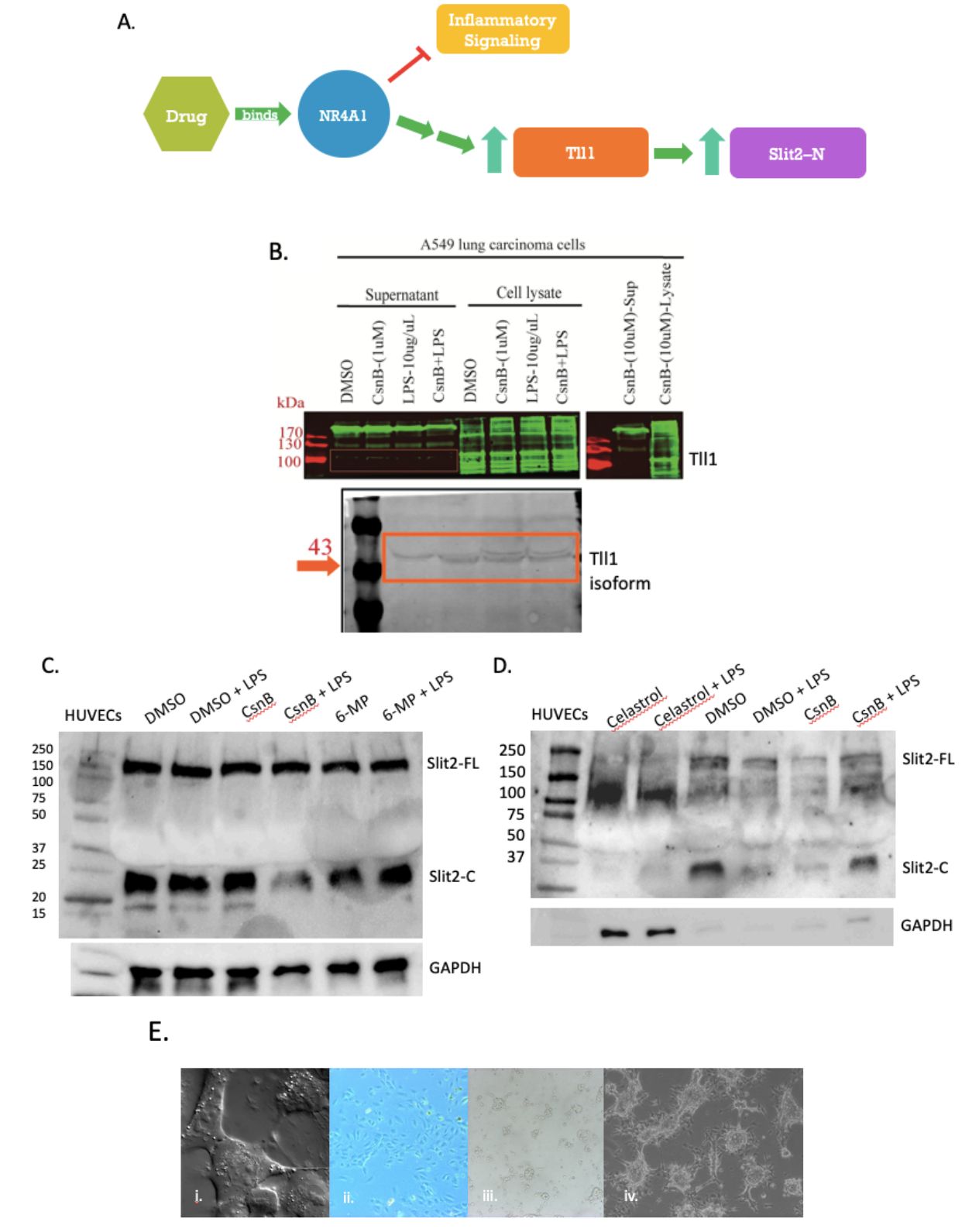
A.
Inflammatory Signaling
Drug
binds
NR4A1
Tll1
Slit2–N
B.
A549 lung carcinoma cells
Supernatant
Cell lysate
DMSO
CsnB-(1uM)
LPS-10ug/uL
CsnB+LPS
DMSO
CsnB-(1uM)
LPS-10ug/uL
CsnB+LPS
CsnB-(10uM)-Sup
CsnB-(10uM)-Lysate
kDa
170
130
100
Tll1
43
Tll1
isoform
C.
HUVECs
DMSO
DMSO + LPS
CsnB
CsnB + LPS
6-MP
6-MP + LPS
250
150
100
75
50
37
25
20
15
Slit2-FL
Slit2-C
GAPDH
D.
HUVECs
Celastrol
Celastrol + LPS
DMSO
DMSO + LPS
CsnB
CsnB + LPS
250
150
100
75
50
37
Slit2-FL
Slit2-C
GAPDH
E.
i.
ii.
iii.
iv.

Figure 2. (A) Slit2-N is a potential therapeutic in virally-mediated inflammatory disease (London et al., 2010). To increase Slit2-N availability, we sought to increase proteolysis of Slit2-FL through indirect upregulation of Tll1 using pharmacological agents. We tested three drugs which agonize NR4A1, a transcription factor associated with high induction of Tll1 (Chao et al, 2008). NR4A1 also modulates proinflammatory signaling (Banno et al, 2019). Pharmacological agents CsnB and Celastrol directly bind NR4A1. 6-MP enhances NR4A1 expression indirectly. **(B-D)** Induction of Tll1 and Slit2 proteolysis was tested using NR4A1 agonist drugs in three different cell types: A549 lung carcinoma cells, mESC-derived glutamatergic neurons (data not shown), and HUVECS. To elicit an immune response mimicking microbial infection, half the samples were treated with LPS which has been shown to robustly upregulate NR4A1 expression in adipocytes (Chao et al, 2008). We predicted greater induction of Tll1 and increased Slit2 proteolysis in LPS treated conditions. **(B)** Western blot of A459 lung carcinoma cell supernatants labeled with a polyclonal antibody for Tll1 shows little to no full-length Tll1 (~114kD). A shorter 43kD isoform was observed and appeared to increase slightly in the presence of CsnB and LPS. This 43kD isoform lacks a catalytic domain so was not pertinent to this study. **(C)** Western blot of HUVEC supernatants labeled with a monoclonal antibody for Slit2-C shows a surprising decrease in Slit2 proteolysis by CsnB in the presence of LPS. Slit2-FL = ~180kD; Slit2-C = ~55kD. **(D)** Western blot of HUVEC supernatants labeled with a monoclonal antibody for Slit2-C shows inverse effect. CsnB in the presence of LPS increased Slit2 proteolysis. DMSO in the absence of LPS appears to have more Slit2 proteolysis than in the presence of LPS. Cytotoxic effects by Celastrol treatment observed by microscopy are demonstrated on the blot by low Slit2 expression and high GAPDH expression. **(E)** Representative images of cell types used in all experiments. All images taken by the author except as indicated. i) A549 lung carcinoma cells (Soong, 2011, WikiMedia), ii) HUVECs, iii) mESC-derived GLUT neurons, and iv) Cos-7 cells.

Drug treatment of A549 Cells

Slit2-N has been identified as potential therapeutic in multiple cell types. We were interested in identifying drugs that would increase the rate of Slit proteolysis (we weren't expecting CMK to do this). A literature search identified Cytosporone B (CsnB) as an agonist of NR4A1, a transcription factor that may induce Tll1 expression (Chao et al, 2008). We tested an additional drug, 6-Mercaptopurine (6-MP) which is an NR4A1 modulator and an FDA-approved drug. For our first experiment in collaboration with Dr. Subhash Verma and Dr. Timsy Uppal we chose to treat A549 lung carcinoma cells due to their high usage in SARS-CoV-2-related studies. Dr.

Uppal raised and treated the cells and together we conducted the Western blots using an antibody against Tll1. To elicit an immune response mimicking microbial infection, we treated half the samples with lipopolysaccharides (LPS). LPS is a pro-inflammatory signal that has also been shown to robustly upregulate NR4A1 expression in adipocytes (Chao et al, 2008). We treated the cells with two concentrations of Can and one concentration of 6-MP. We were unable to detect full-length Tll1 (~114kD) in A549 cells. However, a shorter 43kD isoform of Tll1 was observed and expression of this isoform appeared to increase slightly in the presence of CsnB and LPS (Fig. 2B). Unfortunately, the 43kD isoform lacks a catalytic domain and is likely non-functional. Expression of Slit2-C was not observed in these cells. Due to the inability to observe Slit2 or proteolytically capable Tll1, we chose not to pursue experiments using this cell line.

Drug Treatment in mESC-derived Glutamatergic neurons

In collaboration with Bongmin Bae (Miura Lab), glutamatergic neurons derived from mouse embryonic stem cells (mESCs) were treated with CsnB and 6-MP. We were unable to detect expression of Tll1 or Slit2 in these cells, so could not evaluate drug effects (data not shown; Fig. 2E shows representative image of mESC-derived Glutamatergic neurons used for study).

Drug Treatment in HUVECs

Slit2-N has a documented effect improving vascular stability in cytokine storm, so we chose to investigate human umbilical vein embryonic cells (HUVECs) (London et al., 2010). In collaboration with Dr. Subhash Verma and Dr. Timsy Uppal, HUVECs were treated with CsnB and LPS. Endogenous full-length Tll1 expression was detected at low levels in these cells (data not shown). The relative faintness of the bands makes quantification unreliable, so we were unable to draw any conclusions regarding different levels of Tll1 under different conditions. In contrast, robust endogenous Slit2 expression was detected by Western blot (Fig. 2C, 2D). Surprisingly, in one experiment, CsnB in the presence of LPS appeared to decrease Slit2 proteolysis (Fig. 2C). The combination of an inflammatory stimulus and CsnB decreasing Slit2 proteolysis is the opposite from predicted and in opposition to the desired therapeutic effect. NR4A1 also functions in the cytoplasm and this activity is enhanced by the drug Celastrol, so we repeated the experiment to include Celastrol in addition to CsnB (Huang et al., 2016) Celastrol was toxic to the cells at the concentration used, limiting interpretation of the results (Fig. 2D). However, in this experiment, CsnB and LPS did increase Slit2 processing (Fig. 2D). It appears that Slit2 proteolysis may be amenable to pharmacological regulation, but clearly multiple independent replicates are required before conclusions can be drawn.

Discussion

Contrary to a previous study findings that CMK decreases Slit2 cleavage, we found that, in Cos-7 cells, the prohormone convertase inhibitor CMK instead increased Slit2 proteolysis. We also determined that our activated Tll1 construct appears to be functional in Slit2 processing. Best

demonstrated in HUVECs, we also identified that the NR4A1 agonist drug CsnB has potential to regulate Slit2 proteolysis in the presence of immune response activator LPS, but at this time, no clear conclusion can be drawn.

Previously, the Slit2 cleavage inhibition characteristic of CMK was observed in N2A neuroblastoma cells using a Slit2 construct that was modified with fluorescent proteins fused at either end (considerably larger than standard epitope tags; Ducuing et al, 2020). These differences in cell-type and substrate may have impacted Slit2 processing and contributed to the opposing effect of CMK that we observed. We are interested in repeating our experiment using N2A cells to determine if we can replicate Slit2 cleavage inhibition by CMK in those cells with less altered Slit2 proteins. With the observed effects of CMK opposing the predicted effects, we were not able to definitively exclude or include a Furin-like prohormone convertase as the Slit2 protease, though we continue to suspect that prohormone convertase actions on Slit2 are indirect and relate to activation of Tll1. We plan to repeat our experiment in Cos-7 cells to gain clarity on Slit2 processing in these cells. Replication will help clarify the role of endogenous Slit2 cleavage in this cell line and further characterize the effect of CMK on Slit2 cleavage by Tll1 and aTll1.

Our sequencing and Western blot results clearly demonstrate that we have successfully made an activated Tll1 construct and that it appears to be functional at cleaving Slit2. In fact, it may be over zealous. We observed an increase in Slit2 degradation where aTll was expressed. This kind of substrate degradation by the Slit protease has been well-documented in the Kidd

laboratory, but we have been unable to find examples in the literature. To combat this problem, we reduced the ratio of transfected aTll1 construct and Slit2 construct from 1:1 to 1:4. This helped, but low levels of non-degraded Slit2 full-length and Slit2-C made interpretation of expression difficult to quantify. Optimization to maintain more non-degraded Slit2 expression is ongoing.

We tested the effect of CsnB on Slit2 proteolysis in three distinct cell types: A549 human lung carcinoma cells, mouse embryonic stem cell (mESC)-derived glutamatergic neurons, and human umbilical vein endothelial cells (HUVECs). Due to their detectable Slit2 and Tll1 expression and their value for studying molecular responses in vascular cells, HUVECs proved to be the best cell line for our study. CsnB is a promising candidate drug for therapeutic upregulation of Slit2 proteolysis in the presence of microbial infection mimic LPS, but, due to conflicting results, further investigation is still needed. Between the two other NR4A1 modulator drugs tested, 6-MP and Celastrol, Celastrol is of most continued interest. We are interested in repeating our HUVEC studies with Celastrol at much lower concentration to mitigate toxic effects. Toxicity is a known problem with Celastrol and less toxic derivatives are actively being synthesized.

With over 3 million deaths worldwide from SARS-CoV-2 infection and a 90% incidence of ARDS among those who have died, harnessing the vascular stabilization and inflammation-mediating therapeutic potential of Slit2-N has pressing applications in human health and medicine (Johns Hopkins, 2021, Tzotzos et al., 2020). Accurately identifying the Slit2 protease is imperative for understanding how Slit proteolysis is regulated and determining ways to modulate it.

Pharmacological strategies, like NR4A1 agonism, are a promising approach for increasing Slit2 proteolysis and utilizing the body's own mechanisms to combat SARS-CoV-2-related tissue damage.

Materials & Methods

Activated Tll1 DNA Construct

The template used for the activated Tll1 (aTll1) construct was a human Tll1 clone with a FLAG epitope tag, pcDNA-hTll1-FLAG, which was synthesized by GenScript in the pcDNA3.1+/C-(K)-DYK vector. Consulting Takahara et al. (1996) and Scott et al. (1999), PCR primers were designed to flank the Tll1 inhibitory prodomain and contain 15-bp overlaps at their 5' ends:

TLL1ACTDN: 5' TGGGTCTGCGCTGGCGCCGCTACATCAAGAACG 3'
TLL1ACTUP: 5' GCCAGCGCAGACCCATAGC 3'

The Tll1 construct was amplified by PCR with 2x Taq Red Master Mix (APEX, 5200300-1250; 0.4mM dNTP, 0.08 units/uL Taq, 1 ng DNA per reaction). The In-Fusion Snap Assembly cloning kit (Takara Bio, USA) was used to generate deletions according to the manufacturer's recommended protocol. PCR products were gel-purified and recombined using the NucleoSpin Gel and PCR Clean-Up and In-Fusion Snap Assembly cloning kits (Takara Bio, USA). The recombinant DNAs were transformed into *Escherichia coli* competent cells for screening.

Screening primers were designed to detect if the desired 348bp deletion occurred versus 600bp if undeleted.

T7: 5’ TAATACGACTCACTATAGGG 3’

TLL1ACTSC: 5’ CAAGGCCTATAGGTGAATAC 3’

Constructs were sequenced at the Nevada Genomics Center (UNR) using Sanger sequencing, and the sequences were analyzed in BLAST (blast.ncbi.nlm.nih.gov).

Cos-7 Cell DNA Transfection

COS-7 cells at 80% confluence in a 6-well plate were transfected with DNA expression constructs for Slit2-FL and Tll1 or aTll1 using Lipofectamine 2000 (Life Technologies) in OptiMEM media according to the manufacturer’s instructions. The pSecTag-Slit2-FL-myc-6xHIS construct was obtained from A. Chédotal and is described in Ba-Charvet et al. 2001. The pcDNA-hTll1-FLAG construct which was synthesized by GenScript. As described above, that construct was used as the template for our own synthesis of pcDNA-haTll1-FLAG. A total of 4ug of DNA per well was transfected. In the first experiment, the ratio of Slit2 and Tll1 or aTll1 was 1:1. In the subsequent experiment that ratio was changed to 4:1 to mitigate observed substrate degradation by the protease. The transfection reaction incubated for 4 hours at 37ºC. The media was then replaced with fresh media and the cells were treated with 100uM CMK (EMD

Millipore Corp., 344930). In the first experiment, the replacement media was DMEM (Gibco) with 10% FBS, 1% GlutaMAX (Gibco). Due to the serum interfering with Western blot analysis, we used OptiMEM media which does not contain FBS in the second experiment. The cell supernatants were harvested 48 hours following the media change and CMK treatment.

Drug Treatments of A549 cells, mESC-derived GLUT neurons, and HUVECs

Plated cells at 80% confluence were treated with DMSO (Sigma-Aldrich, 472301) 1uM CsnB (Sigma, C2997), 10uM CsnB (Sigma, C2997), 50uM 6-MP (Sigma, 38171), or 100uM Celastrol (Selleckchem, S1290) plus or minus 10mg/mL LPS (Sigma, L2880). The same drug concentrations were used independent of cell type. The treated cells incubated for 48 hours at 37ºC, then the cell lysates and supernatants were collected.

Antibodies

Cell supernatants were analyzed with SDS-PAGE and the blot was probed with the follow primary antibodies: anti-Slit2-C antibody (rabbit monoclonal, 1:1000, Abcam, ab134166), anti-human Tll1 antibody (rabbit polyclonal, 1:1000, MyBioSource, MBS7049288), and anti-GAPDH antibody (chicken polyclonal, 1:1000, MilliporeSigma, AB2302). Secondary antibodies used were horseradish peroxidase-conjugated goat anti-rabbit (polyclonal, 1:500 Jackson ImmunoResearch, 111-035-003) and horseradish peroxidase-conjugated donkey anti-chicken (polyclonal, 1:500, Jackson ImmunoResearch, 703-035-155). The blots incubated in primary

antibody overnight at 4ºC and in secondary antibody for 1 hour. The blots were then imaged using a ChemiDoc Touch Imaging System. The same antibody formulations and procedures were used across experiments.

Quantification of Slit2 Cleavage and Tll1 Expression

Analysis of Slit cleavage was performed using ImageJ to compare the relative pixel density of Slit-C bands to Slit-FL bands on Western blots after standardizing to GAPDH loading controls. Tll1 expression was also standardized to GAPDH loading controls using pixel density measurements from ImageJ. Quantification analysis reflects individual experimental results and not cross-experiment averages.

References

Alavi, M., Song, M., King, G. L., Gillis, T., Propst, R., Lamanuzzi, M., Bousum, A., Miller, A., Allen, R., & Kidd, T. (2016). Dscam1 Forms a Complex with Robo1 and the N-Terminal Fragment of Slit to Promote the Growth of Longitudinal Axons. *PLoS biology*, *14*(9), e1002560. https://doi.org/10.1371/journal.pbio.1002560

Banno, A., Lakshmi, S. P., Reddy, A. T., Kim, S. C., & Reddy, R. C. (2019). Key Functions and Therapeutic Prospects of Nur77 in Inflammation Related Lung Diseases. *The American journal of pathology*, *189*(3), 482–491. https://doi.org/10.1016/j.ajpath.2018.10.002

Branchfield, K., Nantie, L., Verheyden, J. M., Sui, P., Wienhold, M. D., & Sun, X. (2016). Pulmonary neuroendocrine cells function as airway sensors to control lung immune response. *Science (New York, N.Y.)*, *351*(6274), 707–710. https://doi.org/10.1126/science.aad7969

Brose, K., Bland, K. S., Wang, K. H., Arnott, D., Henzel, W., Goodman, C. S., Tessier-Lavigne, M., & Kidd, T. (1999). Slit proteins bind Robo receptors and have an evolutionarily conserved role in repulsive axon guidance. *Cell*, *96*(6), 795–806. https://doi.org/10.1016/s0092-8674(00)80590-5

Chao, L. C., Bensinger, S. J., Villanueva, C. J., Wroblewski, K., & Tontonoz, P. (2008). Inhibition of adipocyte differentiation by Nur77, Nurr1, and Nor1. *Molecular endocrinology (Baltimore, Md.)*, *22*(12), 2596–2608. https://doi.org/10.1210/me.2008-0161

Delloye-Bourgeois, C., Jacquier, A., Charoy, C., Reynaud, F., Nawabi, H., Thoinet, K., Kindbeiter, K., Yoshida, Y., Zagar, Y., Kong, Y., Jones, Y. E., Falk, J., Chédotal, A., & Castellani, V. (2015). PlexinA1 is a new Slit receptor and mediates axon guidance function of Slit C-terminal fragments. *Nature neuroscience*, *18*(1), 36–45. https://doi.org/10.1038/nn.3893

Ducuing, H., Gardette, T., Pignata, A., Kindbeiter, K., Bozon, M., Thoumine, O., Delloye-Bourgeois, C., Tauszig-Delamasure, S., & Castellani, V. (2020). SlitC-PlexinA1 mediates iterative inhibition for orderly passage of spinal commissural axons through the floor plate. *eLife*, *9*, e63205. https://doi.org/10.7554/eLife.63205

Gonzales, J. N., Lucas, R., & Verin, A. D. (2015). The Acute Respiratory Distress Syndrome: Mechanisms and Perspective Therapeutic Approaches. *Austin Journal of Vascular Medicine*, *2*(1), 1009. https://www.ncbi.nlm.nih.gov/pmc/articles/PMC4786180/

Huang, HY., Chang, HF., Tsai, MJ. *et al.* 6-Mercaptopurine attenuates tumor necrosis factor-α production in microglia through Nur77-mediated transrepression and PI3K/Akt/mTOR signaling-mediated translational regulation. *J Neuroinflammation* 13**,** 78 (2016). https://doi.org/10.1186/s12974-016-0543-5

Jiang, Y., Zeng, Y., Huang, X., Qin, Y., Luo, W., Xiang, S., Sooranna, S. R., & Pinhu, L. (2016). Nur77 attenuates endothelin-1 expression via downregulation of NF-κB and p38 MAPK in A549 cells and in an ARDS rat model. *American journal of physiology. Lung cellular and molecular physiology, 311*(6), L1023–L1035. https://doi.org/10.1152/ajplung.00043.2016

Johns Hopkins University. (2021). *Coronavirus Resource Center.* *https://coronavirus.jhu.edu/map.html*

Jones, C. A., London, N. R., Chen, H., Park, K. W., Sauvaget, D., Stockton, R. A., Wythe, J. D., Suh, W., Larrieu-Lahargue, F., Mukouyama, Y. S., Lindblom, P., Seth, P., Frias, A., Nishiya, N., Ginsberg, M. H., Gerhardt, H., Zhang, K., & Li, D. Y. (2008). Robo4 stabilizes the vascular network by inhibiting pathologic angiogenesis and endothelial hyperpermeability. *Nature medicine*, *14*(4), 448–453. https://doi.org/10.1038/nm1742

Kidd, T., Brose, K., Mitchell, K. J., Fetter, R. D., Tessier-Lavigne, M., Goodman, C. S., & Tear, G. (1998). Roundabout controls axon crossing of the CNS midline and defines a novel subfamily of evolutionarily conserved guidance receptors. *Cell*, *92*(2), 205–215. https://doi.org/10.1016/s0092-8674(00)80915-0

Kidd, T., Bland, K. S., & Goodman, C. S. (1999). Slit is the midline repellent for the robo receptor in Drosophila. *Cell*, *96*(6), 785–794. https://doi.org/10.1016/s0092-8674(00)80589-9

Kellermeyer, R., Heydman, L. M., Gillis, T., Mastick, G. S., Song, M., & Kidd, T. (2020). Proteolytic cleavage of Slit by the Tolkin protease converts an axon repulsion cue to an axon growth cue *in vivo*. *Development (Cambridge, England)*, *147*(20), dev196055. https://doi.org/10.1242/dev.196055

London, N. R., & Li, D. Y. (2011). Robo4-dependent Slit signaling stabilizes the vasculature during pathologic angiogenesis and cytokine storm. *Current opinion in hematology*, *18*(3), 186–190. https://doi.org/10.1097/MOH.0b013e328345a4b9

London, N. R., Zhu, W., Bozza, F. A., Smith, M. C., Greif, D. M., Sorensen, L. K., Chen, L., Kaminoh, Y., Chan, A. C., Passi, S. F., Day, C. W., Barnard, D. L., Zimmerman, G. A., Krasnow, M. A., & Li, D. Y. (2010). Targeting Robo4-dependent Slit signaling to survive the cytokine storm in sepsis and influenza. *Science translational medicine*, *2*(23), 23ra19. https://doi.org/10.1126/scitranslmed.3000678

Nguyen Ba-Charvet, K. T., Brose, K., Ma, L., Wang, K. H., Marillat, V., Sotelo, C., Tessier-Lavigne, M., & Chédotal, A. (2001). Diversity and specificity of actions of Slit2 proteolytic fragments in axon guidance. *The Journal of Neuroscience : the official journal of the Society for Neuroscience*, *21*(12), 4281–4289. https://doi.org/10.1523/JNEUROSCI.21-12-04281.2001

Ordan, E., & Volk, T. (2016). Amontillado is required for Drosophila Slit processing and for tendon-mediated muscle patterning. *Biology open*, *5*(10), 1530–1534. https://doi.org/10.1242/bio.020636

Piper, M., Nurcombe, V., Reid, K., Bartlett, P., & Little, M. (2002). N-terminal Slit2 promotes survival and neurite extension in cultured peripheral neurons. *Neuroreport*, *13*(17), 2375–2378. https://doi.org/10.1097/00001756-200212030-00041

Scott, I. C., Blitz, I. L., Pappano, W. N., Imamura, Y., Clark, T. G., Steiglitz, B. M., Thomas, C. L., Maas, S. A., Takahara, K., Cho, K. W., & Greenspan, D. S. (1999). Mammalian BMP-1/Tolloid-

related metalloproteinases, including novel family member mammalian Tolloid-like 2, have differential enzymatic activities and distributions of expression relevant to patterning and skeletogenesis. *Developmental biology*, *213*(2), 283–300. https://doi.org/10.1006/dbio.1999.9383

Svensson, K. J., Long, J. Z., Jedrychowski, M. P., Cohen, P., Lo, J. C., Serag, S., Kir, S., Shinoda, K., Tartaglia, J. A., Rao, R. R., Chédotal, A., Kajimura, S., Gygi, S. P., & Spiegelman, B. M. (2016). A Secreted Slit2 Fragment Regulates Adipose Tissue Thermogenesis and Metabolic Function. *Cell metabolism*, *23*(3), 454–466. https://doi.org/10.1016/j.cmet.2016.01.008

Takahara, K., Brevard, R., Hoffman, G. G., Suzuki, N., & Greenspan, D. S. (1996). Characterization of a novel gene product (mammalian tolloid-like) with high sequence similarity to mammalian tolloid/bone morphogenetic protein-1. *Genomics*, *34*(2), 157–165. https://doi.org/10.1006/geno.1996.0260

Troilo, H., Bayley, C. P., Barrett, A. L., Lockhart-Cairns, M. P., Jowitt, T. A., & Baldock, C. (2016). Mammalian tolloid proteinases: role in growth factor signalling. *FEBS letters*, *590*(15), 2398–2407. https://doi.org/10.1002/1873-3468.12287

Tzotzos, S. J., Fischer, B., Fischer, H., & Zeitlinger, M. (2020). Incidence of ARDS and outcomes in hospitalized patients with COVID-19: a global literature survey. *Critical care (London, England)*, *24*(1), 516. https://doi.org/10.1186/s13054-020-03240-7

Zhan, Y., Du, X., Chen, H., Liu, J., Zhao, B., Huang, D., Li, G., Xu, Q., Zhang, M., Weimer, B. C., Chen, D., Cheng, Z., Zhang, L., Li, Q., Li, S., Zheng, Z., Song, S., Huang, Y., Ye, Z., Su, W., … Wu, Q. (2008). Cytosporone B is an agonist for nuclear orphan receptor Nur77. *Nature chemical biology*, *4*(9), 548–556. https://doi.org/10.1038/nchembio.106